

---

# Enhancement of the Laser-Induced–Damage Threshold in Multilayer Dielectric Diffraction Gratings Through Targeted Chemical Cleaning

## Introduction

Chirped-pulse amplification (CPA) has been an enabling technology in the development of ultrashort-pulse, high-power laser systems.<sup>1–5</sup> In a CPA setup, a pair of diffraction gratings is used to “chirp” the signal by stretching it in time, reducing the laser pulse to a much lower intensity before the beam travels through the amplifier. The amplified pulse passes through another set of gratings to recompress it to its original pulse duration. At LLE, eight sets of tiled multilayer dielectric (MLD) gratings are used in pulse compressor chambers for OMEGA EP’s two short-pulse beamlines. Each grating segment is 10 cm thick, 47 cm wide, and 43 cm tall; a complete tiled-grating assembly (TGA) is 1.4 m wide and includes three grating segments. The requirements on these critical, large-aperture optics are rigorous: laser-induced damage thresholds greater than 2.7 J/cm<sup>2</sup> (beam normal) for a 10-ps pulse at 1054 nm incident at 61° and a minimum diffraction efficiency of 97%. Because these demands have not yet been met, OMEGA EP’s short-pulse beamlines are currently operated at ~60% of their design energy.

Surface contamination can dramatically reduce a grating’s resistance to laser-induced damage.<sup>5–13</sup> OMEGA EP pulse compressor gratings are fabricated by etching a periodic groove structure (1740 lines/mm) into the top layer of a hafnia/silica multilayer mirror using interference lithography. Optionally, a bottom antireflective coating (BARC) is applied to the multilayer mirror to mitigate standing-wave effects during lithography and to improve fidelity. The grating fabrication process leaves large quantities of manufacturing residues and debris on the grating’s surface that must be removed before the optic can go into service. Residues of hardened organic polymer BARC, in particular, are especially difficult to remove during final grating cleaning. Any photoresist or BARC residues, metal contaminants, surface debris, or light organic matter ultimately left on the grating can absorb energy during laser irradiation, initiating intense local heating and catastrophic laser-induced damage. Therefore, a final grating cleaning process that removes a broad spectrum of contaminant materials is essential. Mechanical contact with the delicate, microtextured

grating surface must be absolutely avoided during cleaning, and cleaning techniques must not be so aggressive that they cause damage or defects. Additionally, short processing times and low temperatures are desirable for practical implementation on large parts and to mitigate thermal stress concerns.

## MLD Grating Cleaning

Although surface contamination is a well-known cause of poor optical performance and laser-damage resistance, relatively few papers on cleaning methods for MLD gratings are available in the literature. Ashe *et al.*<sup>9,10</sup> were among the first to publish on this topic. They compared a number of chemical wet-cleaning methods commonly used in the semiconductor industry. Acid piranha, a mixture of sulfuric acid (H<sub>2</sub>SO<sub>4</sub>) and hydrogen peroxide (H<sub>2</sub>O<sub>2</sub>), was identified as the most-promising chemistry for MLD grating cleaning based on post-cleaning diffraction efficiency (DE) and laser-induced–damage threshold (LIDT) results. Other groups<sup>11–14</sup> have reported on the successful use of acid piranha to clean MLD gratings. Britten and Nguyen<sup>13</sup> developed a cleaning method for diffraction gratings that involved stripping bulk photoresist with an aqueous base and employing an oxidizing acid solution to remove residues; oxygen plasma was used as an intermediate step to remove fluorinated hydrocarbon residues. Plasma cleaning with oxygen and other gases has been suggested as a method for removing bulk organic layers of BARC<sup>9,14</sup> and photoresist<sup>15,16</sup> from gratings.

Britten *et al.*<sup>17,18</sup> demonstrated that briefly exposing an MLD grating to dilute buffered hydrofluoric acid (HF) solution after cleaning could increase resistance to laser-induced damage. HF lightly etches the silica pillars, simultaneously enhancing grating performance by removing surface residues and reducing the duty cycle (linewidth/period). Low duty cycles (tall, thin pillars) can enhance a grating’s LIDT by minimizing electric-field enhancement.<sup>19</sup> Because low-duty-cycle gratings are considerably more difficult to fabricate than those having a traditional surface profile, the discovery of HF linewidth tailoring was a major advancement. The authors reported an average LIDT increase of 18.5% after etchback for 10-ps, 1053-nm damage

testing at  $76.5^\circ$  incidence. Britten *et al.* indicated that the HF linewidth-tailoring treatment “requires densified coating layers,”<sup>18</sup> but did not elaborate.

A few grating cleaning methods<sup>10,17,19</sup> have been shown to meet the OMEGA EP grating LIDT requirement of  $2.7 \text{ J/cm}^2$  for a 1054-nm, 10-ps pulse using small grating samples.<sup>(a)</sup> Attempts to achieve similarly high damage thresholds on full-size OMEGA EP pulse compressor gratings and witness optics have so far been unsuccessful. One problem is that most damage-testing data have been reported for an air environment, while OMEGA EP gratings are operated in high vacuum. The testing environment can have a significant effect on results, especially for nondensified, porous MLD coatings (such as those used by LLE) because humidity and the volatility of contaminant materials in the vacuum chamber can play important roles. A second consideration is that the next generation of OMEGA EP gratings will, preferably, be fabricated with a BARC layer over the multilayer stack to minimize interference effects and distortion of the grating line structures at low duty cycles. Since many grating manufacturers do not use BARC, little information is available on stripping it from MLD gratings during final cleaning. Finally, wet-cleaning of MLD gratings has typically been performed at high temperatures ( $60^\circ\text{C}$  to  $110^\circ\text{C}$ ), especially when acid piranha is used to strip photoresist.<sup>9–12</sup> Such elevated processing temperatures have recently raised concerns about thermal-stress-induced defects, such as blistering and localized coating delamination, that can occur during cleaning. Two examples of coating failure observed in our lab on hafnia/silica MLD’s and MLD gratings following elevated-temperature cleaning are given in Fig. 131.9. Figure 131.9(a) shows a group of  $\sim 40\text{-}\mu\text{m}$ -diam “blister” defects that nucleated near scratches on an MLD during piranha cleaning at  $90^\circ\text{C}$ . Figure 131.9(b) is a tiled micrograph showing localized delamination of an MLD grating after piranha cleaning at  $70^\circ\text{C}$ . To compound concerns about thermal stresses, the behavior of small witness gratings may not be representative of full-scale pulse compressor gratings. Large optics may be susceptible to modes of thermal-stress-induced failure not predicted by small witness parts.<sup>20</sup>

To resolve the above issues, we sought a grating cleaning process that (1) meets OMEGA EP’s specifications for DE and in-vacuum LIDT; (2) is compatible with standard, nondensified reactive-evaporation MLD coatings; (3) effectively strips both

<sup>(a)</sup>Only Ashe<sup>10</sup> reported LIDT data for  $61^\circ$  beam incidence (OMEGA EP specification). Neauport’s<sup>19</sup> and Nguyen’s<sup>17</sup> data were reported for  $77.2^\circ$  and  $76.5^\circ$  incidences, respectively.

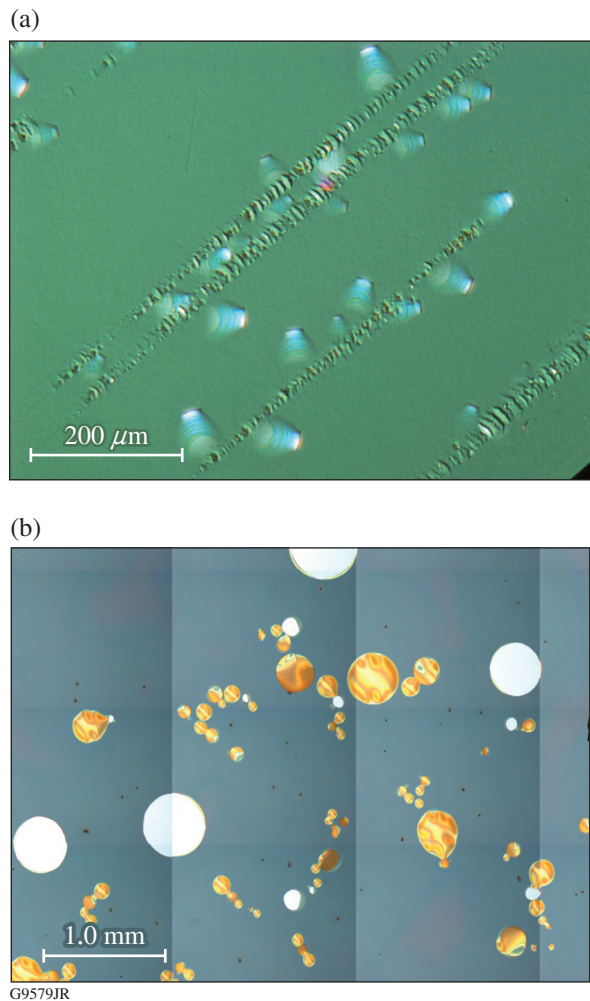


Figure 131.9

Coating failure observed after elevated-temperature acid piranha cleaning: (a) formation of “blister” defects observed on a multilayer dielectric (MLD) coating (no grating) after acid piranha cleaning at  $90^\circ\text{C}$ ; (b) localized delamination observed on an MLD grating after acid piranha cleaning at  $70^\circ\text{C}$ .

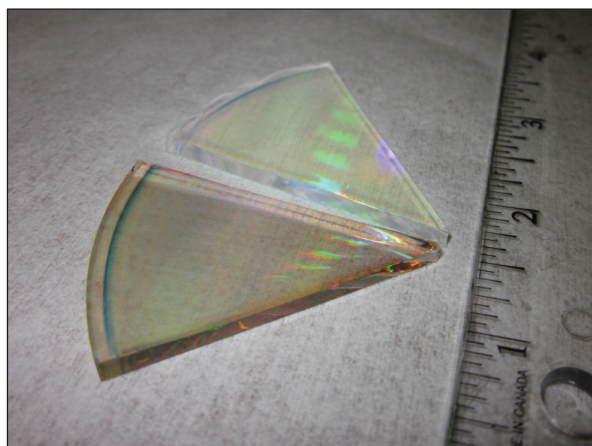
photoresist and BARC; and (4) requires no chemical processing at temperatures above  $40^\circ\text{C}$ , to reduce thermal-stress concerns.

## Experimental

### 1. MLD Grating Samples

Cleaning experiments were performed on small-scale MLD grating coupons. Ten 100-mm-diam, 3-mm-thick, round hafnia/silica MLD gratings were broken into eight equally sized, wedge-shaped coupons (80 samples total). Figure 131.10 shows the sample geometry. The multilayer coating was a modified quarter-wave thin-film stack<sup>21</sup> with hafnia ( $\text{HfO}_2$ ) and silica ( $\text{SiO}_2$ ) used as the high- and low-index materials, respectively. The total coating thickness was  $4.8 \mu\text{m}$ . The MLD was deposited by reactive evaporation at  $150^\circ\text{C}$  using oxygen backfill

pressures of  $2.0 \times 10^{-4}$  Torr for hafnia deposition and zero for silica layer deposition. A BARC layer was applied over the multilayer to mitigate interference effects during photolithography. Grooves (1740 lines/mm) were etched into the top silica layer of the MLD. The samples were “identical” in that they were produced in the same coating run and processed together up until the final cleaning stage. Except as noted, all cleaning experiments described in this article were performed on *uncleaned* gratings with BARC and photoresist still intact (that is, they were not subjected to any photoresist stripping or other cleaning operations other than those described here).



G9650JR

Figure 131.10  
Grating wedge samples used in cleaning experiments, shown before (bottom) and after cleaning (top).

## 2. Laser-Induced-Damage Testing

Damage testing was performed at LLE’s Damage Testing Facility on the short-pulse (10-ps) system, which can be operated in both air and high-vacuum ( $4 \times 10^{-7}$  Torr) environments. MLD grating samples were tested using *s*-polarized light at 1054 nm, with an incident beam angle of  $61^\circ$  and an irradiation spot size of  $370 \mu\text{m}$  ( $e^{-1}$  in intensity) in the far field. Laser-damage assessment was performed *in situ* using a white-light imaging system ( $\sim 100\times$  magnification). Damage was defined as a feature on the sample’s surface that was not observed before laser irradiation. When switching between testing environments, samples were allowed to reach equilibrium with the environment (air or vacuum) for 24 h before testing continued. Damage thresholds are reported as beam normal fluences.

Each sample was tested in both 1-on-1 and *N*-on-1 testing regimes. The 1-on-1 damage threshold is determined by irradiating a sample site with one pulse and observing the sample

for damage. This is then repeated with increasing fluences on nonirradiated sample sites until damage is observed. The 1-on-1 threshold is the average of the fluence for the last site that did *not* damage the sample and the fluence for the first site that *did* damage, and the measurement error recorded is half the difference between these two numbers. *N*-on-1 damage testing is conducted by irradiating the sample site at a fluence significantly below the 1-on-1 threshold for ten shots. If no damage is detected, the fluence is increased and the same site is irradiated with five more shots. If no damage is observed after these shots, the fluence is increased again and another five shots are taken. This is continued until damage is observed in white light, at which point the damage onset fluence is recorded as the *N*-on-1 threshold for that site. The *N*-on-1 test is repeated for five sites on each MLD grating sample to generate an average and a standard deviation, which are reported as the *N*-on-1 threshold and measurement error, respectively.

## 3. Acid Piranha Cleaning at Low Temperatures

Many of the techniques used to clean MLD gratings have been developed from methods used for wafer cleaning in the semiconductor industry. Acid piranha, for example, has been known as a photoresist stripper since at least 1975 (Ref. 22), and its use is prevalent in the semiconductor industry. Standard operating procedure for acid piranha varies, but typical acid/peroxide ratios are in the range 2:1 to 7:1 (2 to 7 parts 99% sulfuric acid to 1 part 30% hydrogen peroxide) and typical processing temperatures are in the range  $90^\circ\text{C}$  to  $140^\circ\text{C}$  (Refs. 23 and 24). Optimized piranha-cleaning processes for MLD gratings documented in the open literature have been consistent with these ranges.<sup>10–12</sup> Ashe *et al.*<sup>10</sup> found that laser-damage resistance was maximized when high cleaning temperatures were used and when the proportion of  $\text{H}_2\text{O}_2$  in the piranha solution was high. Piranha 2:1 (two parts sulfuric acid, one part hydrogen peroxide) at  $100^\circ\text{C}$  gave the best LIDT results. The authors recorded *N*-on-1 damage thresholds as high as  $3.27 \text{ J/cm}^2$  in air after piranha cleaning—exceeding the OMEGA EP pulse compressor grating performance specification of  $2.7 \text{ J/cm}^2$ . Thresholds above  $2.7 \text{ J/cm}^2$ , however, were observed only for grating samples cleaned at temperatures of  $80^\circ\text{C}$  or higher, and these were in-air values only.

Because of thermal stress concerns, we chose to work at temperatures of  $40^\circ\text{C}$  or below. Table 131.I shows cleaning parameters and post-cleaning DE and LIDT results for a group of grating samples cleaned for 30 min at  $40^\circ\text{C}$  in an acid piranha bath. Some experiments involved two piranha treatments. This methodology was motivated by Beck *et al.*,<sup>22</sup> who suggested a two-step photoresist strip that employed first

Table 131.I: Treatments and results for 30-min acid piranha soak cleaning experiments, illustrating that acid piranha alone does not clean MLD gratings effectively at 40°C.

Part ID	Ratio H <sub>2</sub> SO <sub>4</sub> :H <sub>2</sub> O <sub>2</sub> /duration		Cleaning temperature	Post-cleaning DE	Post-cleaning LIDT (J/cm <sup>2</sup> ) in vacuum	
	Treatment 1	Treatment 2			1-on-1	N-on-1
555-2	10:1/15 min	5:1/15 min	40°C	84.6±0.8%	0.66±0.01	0.97±0.03
555-1	5:1/15 min	2:1/15 min	40°C	91.7±1.5%	0.84±0.06	1.08±0.11
555-6	10:1/30 min		40°C	90.8±1.2%	0.76±0.02	1.00±0.05
555-5	5:1/30 min		40°C	81.3±1.0%	0.94±0.05	1.04±0.04
555-3	2:1/30 min		40°C	91.0±1.6%	0.95±0.04	1.08±0.06

an acid-rich dehydrating bath, followed by a peroxide-rich oxidizing bath, to exploit the complementary material-removal mechanisms of acid piranha (dehydration and oxidation).

The experiments clearly demonstrated that at these low temperatures, acid piranha cleaning was inadequate. During damage testing, the unamplified laser beam used for alignment “wrote a track” onto the grating as it scanned across the samples, indicating that photoresist was not completely removed. A scanning electron microscope (SEM) observation of sample #555-5 (5:1 piranha, 30 min, 40°C) revealed intact photoresist over the entire grating surface. In areas irradiated during damage testing, the photoresist was deformed and/or stripped away, as shown in Fig. 131.11. The laser treatment provided a “cleaning” effect in the center of the damage site, where the photoresist was entirely removed by the incident laser beam. Near the edges of the region there was significant scatter from partially removed, deformed, and peeling strands of photoresist.

#### 4. Targeted Chemical Cleaning

While acid piranha may be an effective solitary cleaning chemistry for MLD gratings at high temperatures, such was not our experience at 40°C. The intentionally low processing temperature necessitated a new approach. Because gratings are sensitive to surface pollutants of many different types, we developed a multistep technique to ensure broadband removal of performance-limiting contaminants. Cleaning techniques were adapted and combined from various sources to develop the optimized method detailed in Table 131.II. Drawn from semiconductor wafer processing and grating cleaning literature, the references describe other applications for each cleaning technique.

The cleaning process includes six major steps: First, acid piranha is used to strip photoresist and BARC. The piranha strip is followed by plasma cleaning in room air to clear away partially removed BARC and photoresist. Microscopic

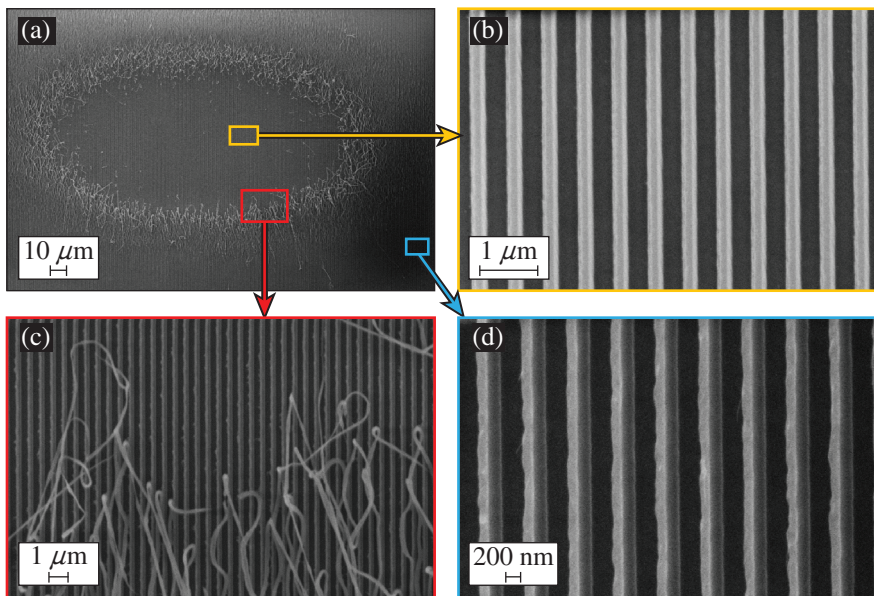


Figure 131.11

Scanning electron microscope (SEM) images of damage site on sample #555-5 irradiated at 1.40 J/cm<sup>2</sup> (1-on-1, 1054 nm, 10 ps, in vacuum, 61° incidence): (a) entire damage site; (b) intact pillars at center of site where all photoresist has been removed via laser irradiation (“cleaning” effect); (c) photoresist peeling away from pillars near the edge of the central region; (d) grating pillars near the edge of the damage site, where the photoresist layer is tilted over and partially detached from the grating pillars due to the 61° incident angle of the laser beam.

G9651JR

Table 131.II: Optimized cleaning method.

Process	Purpose	Method	Chemistry	Duration	Temperature
1. Piranha strip (Refs. 9–12, 22–24)	Strips/softens photoresist and BARC.	Spray onto optic; DI water rinse	H <sub>2</sub> SO <sub>4</sub> :H <sub>2</sub> O <sub>2</sub> (5:1, 2:1)	5:1/15 min, 2:1/15 min	40° to 70°C
2. Plasma clean (Refs. 13,15, 16,23,24)	Removes light organics and partially removed material.	Room air used as process gas	n/a	10 min	Room temperature
3. Ionic clean (SC-2) (Refs. 23,24)	Eliminates remaining ionic/metallic contamination.	Beaker soak; DI water rinse	HCl:H <sub>2</sub> O <sub>2</sub> :H <sub>2</sub> O (1:1:6)	10 min	40° to 70°C
4. Plasma clean (Refs. 13,15, 16,23,24)	Removes light organics and partially removed material.	Room air used as process gas	n/a	10 min	Room temperature
5. Oxide etch (Refs. 18, 23,24)	Removes a thin layer of SiO <sub>2</sub> along with any stubbornly adhered contaminants; thins pillars slightly, reducing duty cycle.	Beaker soak; DI water rinse	HF:buffers (1:2500 to 1:3000)	5 min	Room temperature
6. Plasma clean (Refs. 13,15, 16,23,24)	Removes light organics and partially removed material.	Room air used as process gas	n/a	10 min	Room temperature

examination of samples suggested that BARC flakes off rather than gradually dissolving in piranha solution, and the plasma treatment ensures that material has been completely removed before proceeding to the next cleaning step. The third step in the cleaning process is an ionic clean with a Standard Clean 2 (SC-2) solution, a mixture of hydrochloric acid and hydrogen peroxide commonly used in the microelectronics industry to remove metallic contamination from silicon wafers. The inclusion of an ionic clean was motivated by the detection of molybdenum, a metal, on grating samples (see the next section). The ionic clean is followed by a second plasma treatment to clear away light organic matter collected on the sample. The next step is the oxide etch, which reduces the grating duty cycle and eliminates any remaining contaminants on the grating by removing a thin layer of silica.<sup>17</sup> Grating performance was quite sensitive to the concentration of the buffered oxide etch used. We found that dilutions in the range of 2500 to 3000 parts water/buffers to one part hydrofluoric acid were optimal for a 5-min etch (results discussed later in this section). The final step is a third air plasma treatment, which cleans the surface by removing light organics.

A total of 14 grating samples were cleaned according to the process steps shown in Table 131.II. The samples were then evaluated for damage threshold and diffraction efficiency; results are listed in Table 131.III. Average in-air damage thresholds were 4.01 J/cm<sup>2</sup> and 3.40 J/cm<sup>2</sup> in the 1-on-1 and *N*-on-1 regimes, respectively. For the five samples tested in a vacuum environment, average damage thresholds were 3.36 J/cm<sup>2</sup> (1-on-1) and 2.76 J/cm<sup>2</sup> (*N*-on-1) for 10-ps pulses at

1054 nm in vacuum. The data show good repeatability. For all samples except for the one having the lowest LIDT (562-7), the 1-on-1 threshold exceeded the *N*-on-1 threshold. This is not a typical result. *N*-on-1 thresholds are generally higher because contamination and debris on the grating surface are cleared away by low-fluence laser shots as beam fluence is ramped up, an effect known as “laser conditioning.”<sup>5</sup> The absence of a laser-conditioning effect for the samples cleaned using the optimized method indicates that these gratings were already quite clean when damage testing began.

To our knowledge, this is the first time laser-induced-damage thresholds exceeding the OMEGA EP requirement of 2.7 J/cm<sup>2</sup> *in vacuum* have been reported for MLD gratings. These may also be the highest-reported 10-ps, 1054-nm damage thresholds for gratings fabricated using BARC. The average DE was 97.6%, meeting the OMEGA EP requirement on grating diffraction efficiency. Figure 131.12 compares SEM cross sections of a grating sample before and after cleaning, showing that BARC and photoresist were completely removed and that pillars were slightly narrowed.

The steps shown in Table 131.II were optimized using the set of 80 grating samples described in **MLD Grating Samples** (p. 150). Damage thresholds were found to be especially sensitive to the dilution of HF used in the oxide etch step. As shown in Fig. 131.13, LIDT results were best for grating samples prepared using buffer:HF ratios in the range 2500:1 to 3000:1. An 1800:1 ratio (not shown) led to total delamination of the grating MLD during the 5-min etch.

A major advantage of the targeted cleaning approach is its effectiveness at low temperatures. Lower temperatures lessen

concerns about thermal stresses and reduce susceptibility to blistering and delamination defects. Initial piranha-cleaning experiments at low temperatures (see **Acid Piranha Cleaning at Low Temperatures**, p. 151) suggested that at temperatures

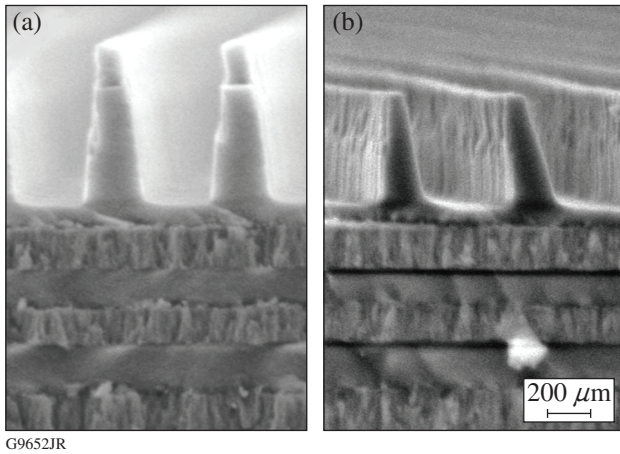


Figure 131.12 SEM images showing MLD grating cross section (a) before chemical cleaning, with BARC and photoresist layers intact and (b) after cleaning, with BARC and photoresist stripped and grating pillars narrowed.

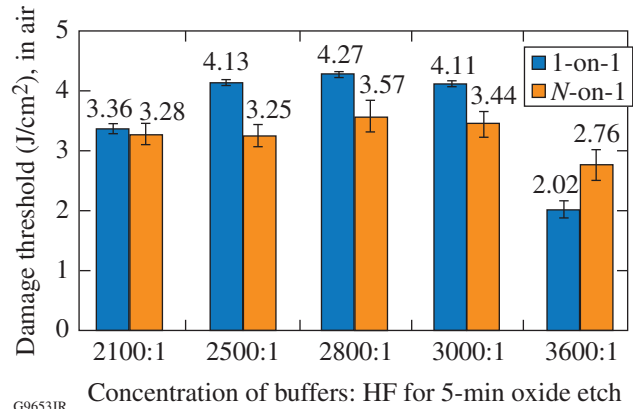


Figure 131.13 Effect of oxide etch concentration on laser-induced-damage threshold of MLD gratings.

Table 131.III: LIDT and DE results for grating samples cleaned using the optimized method.

Part ID	HF dilution (HF:buffers)	Cleaning temperature (piranha strip, ionic clean)	Post-cleaning DE	Post-cleaning LIDT (J/cm <sup>2</sup> ) in air		Post-cleaning LIDT (J/cm <sup>2</sup> ) in vacuum	
				1-on-1	N-on-1	1-on-1	N-on-1
562-6	2500:1	40°C	98.1±0.4%	4.40±0.17	3.49±0.17	3.30±0.19	2.74±0.14
566-1	2800:1	40°C	97.3±0.4%	3.87±0.13	3.32±0.18		
566-2*	2800:1	40°C	97.4±0.5%	3.32±0.13	3.20±0.12		
564-8**	2800:1	40°C	97.4±0.2%	4.24±0.18	3.44±0.21		
562-7	2500:1	50°C	97.4±0.4%	3.11±0.10	3.19±0.19	3.32±0.02	2.69±0.07
566-6	2800:1	50°C	97.4±0.5%	3.90±0.12	3.51±0.07		
557-2***	2800:1	50°C	96.4±0.7%	4.50±0.08	3.55±0.26	3.29±0.10	2.66±0.07
566-7	2800:1	60°C	97.5±0.3%	3.91±0.15	3.33±0.18		
555-5***	3000:1	60°C	97.0±0.3%	4.11±0.05	3.44±0.21		
564-7*	2500:1	70°C	98.7±0.3%	4.25±0.16	3.54±0.12		
564-6**	2500:1	70°C	97.6±0.3%	4.28±0.20	3.06±0.25		
562-3	2500:1	70°C	97.0±0.3%	4.07±0.01	3.39±0.10	3.19±0.16	2.90±0.04
566-8	2800:1	70°C	98.3±0.5%	3.89±0.20	3.56±0.31	3.70±0.16	2.82±0.20
555-2***	2800:1	70°C	97.8±0.4%	4.27±0.05	3.57±0.26		
Average (14 samples)			97.6%	4.01	3.40	3.36	2.76
Standard deviation (14 samples)			0.55%	0.40	0.16	0.20	0.10

\*Piranha 2:1 only (30 min)

\*\*Piranha 5:1 only (30 min)

\*\*\*A re-used grating sample was used for this experiment. The earlier cleaning experiment did not remove photoresist/BARC.

of 40°C and below, acid piranha could not remove BARC and photoresist from an MLD grating. The cleaning approach shown in Table 131.II is much less temperature sensitive. Figure 131.14 shows in-air damage testing results for six samples cleaned using the optimized method at cleaning temperatures ranging from room temperature to 70°C. Differences in damage threshold results for the four samples cleaned in the range of 40°C to 70°C were not statistically significant, suggesting that cleaning temperatures can be safely reduced to the goal temperature of 40°C without negatively impacting grating performance.

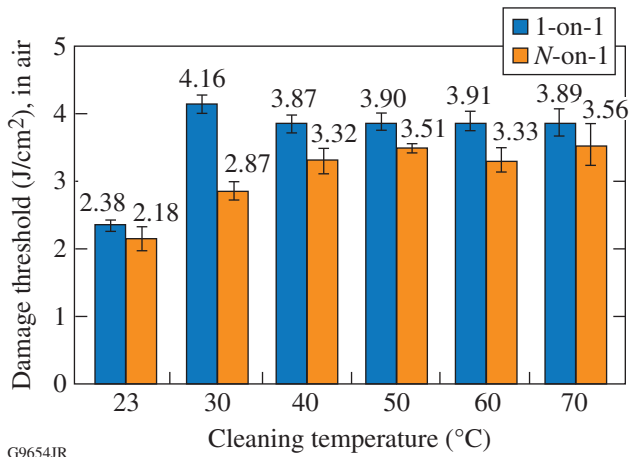


Figure 131.14 Relationship between in-air LIDT and cleaning temperature.

A unique aspect of the grating cleaning process shown in Table 131.II is the use of room air as the process gas in our plasma-cleaning setup. Plasmas generated from oxygen gas (O<sub>2</sub>) are more commonly used.<sup>13-16</sup> We found oxygen plasma to be over aggressive, however, and using room air provides a gentler alternative. Figure 131.15 compares plasma-cleaning results for the two process gases. Grating samples were initially cleaned according to the method of Table 131.II and then plasma cleaned for 1, 3, 5, or 10 min using either oxygen or room air as the process gas in a Harrick PDC-32G plasma cleaner. All samples treated with room-air plasma saw an increase in diffraction efficiency (average, +0.43%) and met the OMEGA EP specification of 97% after cleaning, while all samples treated with oxygen plasma saw a drop in DE (average, -0.63%) and only two of four met the OMEGA EP specification. Shorter treatment times (15 and 30 s) were considered for oxygen plasma. The 15-s treatment improved diffraction efficiency modestly (+0.45%), but precise timing was a challenge for such short process durations because initial adjustments to generate a stable plasma require several seconds. The 30-s

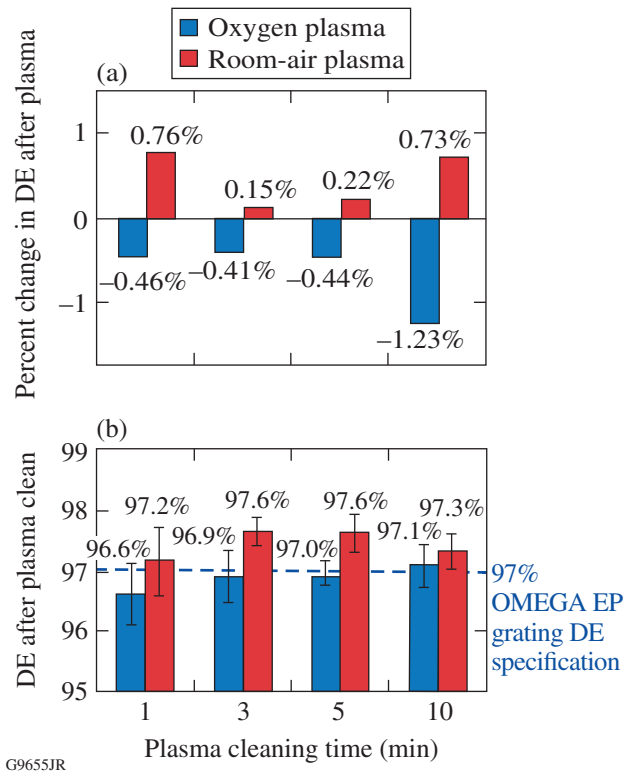


Figure 131.15 Comparison of oxygen and room-air plasma cleaning at room temperature. (a) Oxygen plasma cleaning for 1 to 10 min had a negative effect on diffraction efficiency, whereas room-air plasma cleaning enhanced DE. (b) All four samples treated with room-air plasma exceeded the 97% OMEGA EP grating DE specification, while only two of the four samples treated with oxygen plasma met this specification.

treatment had a negative effect on DE (-0.39%). Because room-air plasma was gentler, process control was superior because cleaning times could be longer.

Room-air plasma was found to be useful in “cleaning up” grating surfaces that failed to meet DE specifications after initial cleaning. Figure 131.16 shows the effect of a 15-min plasma treatment on three piranha-cleaned samples having initially poor diffraction efficiencies. Each of the three samples was improved from 86% to 87% to greater than 95% efficiency. We hypothesize that the air plasma treatment cleared away BARC and photoresist material that may have been softened or been partially removed in previous cleaning steps. Air plasma cleaning is effective at removing organic materials accumulated on the surface during storage and handling. In the optimized clean (Table 131.II), a plasma treatment is included after each wet-processing step to ensure that contaminants introduced (or partially removed) during previous cleaning steps are stripped away before moving on to the next cleaning phase.

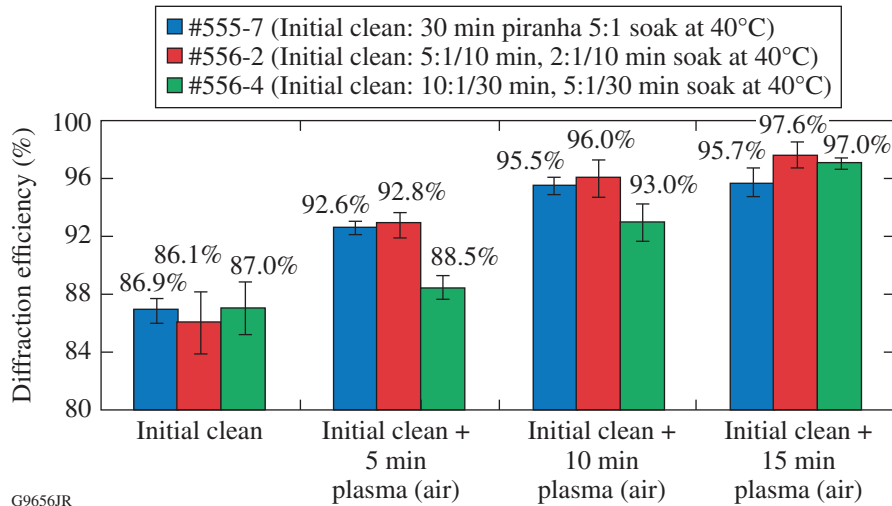


Figure 131.16

Diffraction efficiency enhancement of MLD gratings after room-air plasma cleaning.

G9656JR

### 5. X-Ray Photoelectron Spectroscopy Results

X-ray photoelectron spectroscopy (XPS) was used to evaluate the composition of materials on the grating surface at different phases in the cleaning process. Grating samples were prepared according to Table 131.II, with acid piranha and ionic cleaning steps performed at 70°C and an HF ratio of 3000:1. A piece of grating was reserved for XPS analysis after each process. XPS testing was performed by the Penn State Materials Characterization Lab (sample #555-4), the University of Dayton Research Institute (samples #562-4A, #562-4B, #562-4C, and #562-4D), and the Cornell Center for Materials Research (sample #555-5). Identically prepared samples were also submitted for laser-induced-damage testing. Results are shown in Table 131.IV.

Since the top layer of the grating is SiO<sub>2</sub>, the “ideal” XPS result for a well-cleaned grating would be 33% Si, 67% O, and

nothing else. However, because samples are quickly contaminated with organic materials from the environment, some carbon is also expected. The detection of other elements (or large amounts of carbon) is undesirable and indicates insufficient removal of BARC, photoresist, and/or contaminants. In addition to silicon and oxygen (from the SiO<sub>2</sub> top layer), 42% carbon, 8% fluorine, and 3% molybdenum were detected on the uncleaned grating sample (#555-4). Much of the carbon is attributed to the organic photoresist/BARC layers still intact on the part. Fluorine contamination most likely occurred during reactive-ion beam etching of the grating’s groove structure, as has been reported by others.<sup>9,11,12</sup> The detection of molybdenum was surprising and motivated the inclusion of a hydrochloric-acid-based ionic cleaning step to specifically target metallic contamination (see Table 131.II). The ionic clean may also remove trace contaminants such as potassium, sodium, chromium, iron, and aluminum. While not identified in XPS scans of our grating

Table 131.IV: Elements detected on MLD gratings at various stages of cleaning and corresponding damage-testing results.

Processing	Sample ID (XPS)	Elements detected by XPS (at. %)							Sample ID (damage testing)	LIDT <i>in air</i> (J/cm <sup>2</sup> )	
		O	Si	C	F	Mb	Hf	N		1-on-1	N-on-1
Uncleaned	555-4	35.2	12.0	41.8	8.00	2.60	–	–	555-4	<0.13	
Piranha	562-4A	45.6	16.4	32.4	1.63	–	–	4.0	560-3	1.41±0.06	1.87±0.11
Piranha + plasma	562-4B	60.3	26.7	13.1	–	–	–	–	560-3	2.13±0.11	2.27±0.09
Piranha + plasma + ionic clean	562-4C	61.0	26.6	12.4	–	–	–	–	560-3	2.28±0.05	2.45±0.12
Piranha + plasma + ionic clean + plasma	562-4D	61.3	26.8	11.9	–	–	–	–	560-3	2.13±0.04	2.34±0.13
Piranha + plasma + ionic clean + plasma + oxide etch + plasma	555-5	60.1	23.8	14.2	–	–	1.0	1.0	555-5	4.11±0.05	3.44±0.21



samples, Ashe *et al.*<sup>9,10</sup> detected these ions on similarly prepared MLD grating samples using the much more sensitive ToF-SIMS (time-of-flight secondary ion-mass spectrometry) technique. Metals absorb strongly at 1054 nm, so damage resistance is quite sensitive to this type of contaminant.

After the piranha and plasma treatments, fluorine and molybdenum levels were below the XPS detection limit and carbon levels had dropped to 13.1%. The biggest drop in carbon level occurred after the plasma treatment (rather than the piranha step), supporting our hypothesis that room-air plasma strips partially removed BARC and photoresist. The remaining cleaning steps (ionic clean, plasma, oxide etch, and plasma) did not have significant effects on the XPS spectra. Figure 131.17 shows contaminants detected side-by-side with LIDT results. After bulk removal of photoresist and BARC, XPS may not be sensitive enough to identify trace contaminants that limit resistance to laser-induced damage.

### Conclusions

A low-temperature cleaning method was developed to remove manufacturing residues from MLD pulse-compressor gratings manufactured with polymer BARC. The process,

which is effective at processing temperatures as low as 40°C, targets specific families of contaminants in a sequence of cleaning operations. Samples cleaned using the optimized method had outstanding performance: laser-induced-damage thresholds averaged 4.01 J/cm<sup>2</sup> in air and 3.36 J/cm<sup>2</sup> in vacuum (1-on-1 testing regime, 10 ps, 1054 nm, 61°), and average diffraction efficiency was 97.6%.

### ACKNOWLEDGMENT

This work was supported by the U.S. Department of Energy Office of Inertial Confinement Fusion under Cooperative Agreement No. DE-FC52-08NA28302, the University of Rochester, and the New York State Energy Research and Development Authority. The support of DOE does not constitute an endorsement by DOE of the views expressed in this article.

### REFERENCES

1. L. J. Waxer, D. N. Maywar, J. H. Kelly, T. J. Kessler, B. E. Kruschwitz, S. J. Loucks, R. L. McCrory, D. D. Meyerhofer, S. F. B. Morse, C. Stoeckl, and J. D. Zuegel, *Opt. Photonics News* **16**, 30 (2005).
2. D. Strickland and G. Mourou, *Opt. Commun.* **56**, 219 (1985).
3. G. A. Mourou, in *Encyclopedia of Modern Optics*, edited by R. D. Guenther, D. G. Steel, and L. P. Bayvel (Elsevier Academic Press, Amsterdam, 2005), pp. 83–84.

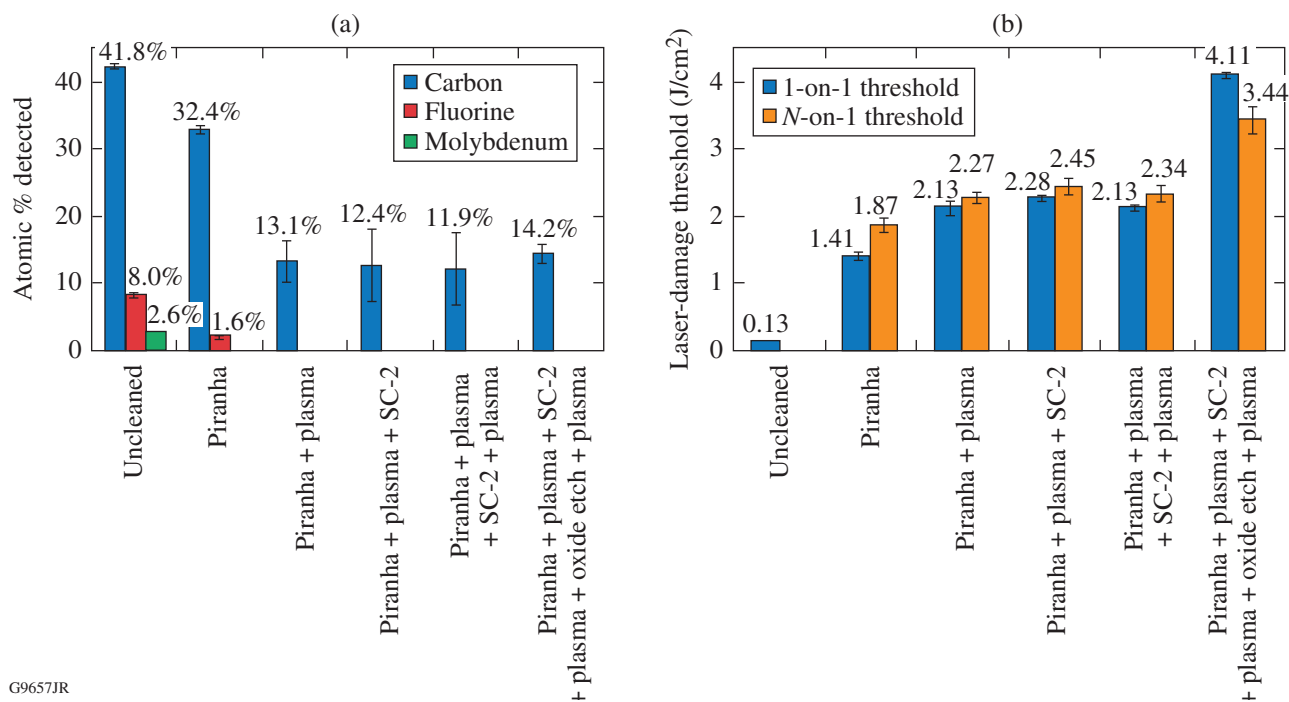


Figure 131.17

(a) Levels of carbon, fluorine, and molybdenum detected after each cleaning step; (b) corresponding laser-induced-damage thresholds.

4. J. A. Britten *et al.*, in *Laser-Induced Damage in Optical Materials: 1995*, edited by H. E. Bennett *et al.* (SPIE, Bellingham, WA, 1996), Vol. 2714, pp. 511–520.
5. I. Jovanovic *et al.*, in *Laser-Induced Damage in Optical Materials: 2004*, edited by G. J. Exarhos *et al.* (SPIE, Bellingham, WA, 2005), Vol. 5647, pp. 34–42.
6. B. Ashe, K. L. Marshall, D. Mastrosimone, and C. McAtee, in *Optical System Contamination: Effects, Measurements, and Control 2008*, edited by S. A. Straka (SPIE, Bellingham, WA, 2008), Vol. 7069, p. 706902.
7. W.-J. Kong *et al.*, *Chin. Phys. Lett.* **22**, 1757 (2005).
8. W. Kong *et al.*, *Microelectron. Eng.* **83**, 1426 (2006).
9. B. Ashe, K. L. Marshall, C. Giacomini, A. L. Rigatti, T. J. Kessler, A. W. Schmid, J. B. Oliver, J. Keck, and A. Kozlov, in *Laser-Induced Damage in Optical Materials: 2006*, edited by G. J. Exarhos *et al.* (SPIE, Bellingham, WA, 2007), Vol. 6403, p. 640300.
10. B. Ashe, C. Giacomini, G. Myhre, A. W. Schmid, in *Laser-Induced Damage in Optical Materials: 2007*, edited by G. J. Exarhos *et al.* (SPIE, Bellingham, WA, 2007), Vol. 6720, p. 67200N.
11. S. Chen *et al.*, *High Power Laser Part. Beams* **23**, 2106 (2011).
12. S. Chen *et al.*, in *5th International Symposium on Advanced Optical Manufacturing and Testing Technologies: Advanced Optical Manufacturing Technologies*, edited by L. Yang *et al.* (SPIE, Bellingham, WA, 2010), Vol. 7655, p. 765522.
13. J. A. Britten *et al.*, U.S. Patent Application No. US 2008/0062522 A1 (13 March 2008).
14. B. Xu *et al.*, in *Proceedings of the 50th Annual Technical Conference of the Society of Vacuum Coaters* (Society of Vacuum Coaters, Louisville, KY, 2007), pp. 369–376.
15. Y. Hong *et al.*, *Vacuum* **45**, 25 (2008).
16. A. Bodere *et al.*, *Mater. Sci. Eng. B* **28**, 293 (1994).
17. H. T. Nguyen, C. C. Larson, and J. A. Britten, in *Laser-Induced Damage in Optical Materials: 2010*, edited by G. J. Exarhos *et al.* (SPIE, Bellingham, WA, 2010), Vol. 7842, p. 78421H.
18. J. Britten, C. Larson, M. Feit, and H. Nguyen, presented at the ICUIL 2010 Conference, Watkins, Glen, NY, 26 September–1 October 2010.
19. J. Neauport *et al.*, *Opt. Express* **15**, 12508 (2007).
20. H. Howard, J. C. Lambropoulos, and S. Jacobs, in *Optical Fabrication and Testing*, OSA Technical Digest (online) (Optical Society of America, Washington, DC, 2012), Paper OW3D.3.
21. J. B. Oliver, T. J. Kessler, H. Huang, J. Keck, A. L. Rigatti, A. W. Schmid, A. Kozlov, and T. Z. Kosci, in *Laser-Induced Damage in Optical Materials: 2005*, edited by G. J. Exarhos *et al.* (SPIE, Bellingham, WA, 2005), Vol. 5991, pp. 402–408.
22. W. Beck *et al.*, U.S. Patent No. 3,900,337 (19 August 1975).
23. G. W. Gale, R. J. Small, and K. A. Reinhardt, in *Handbook of Silicon Wafer Cleaning Technology*, 2nd ed., edited by K. A. Reinhardt and W. Kern, Materials Science & Process Technology Series (William Andrew, Norwich, NY, 2008), pp. 201–265.
24. D. W. Burns, in *MEMS Materials and Processes Handbook*, edited by R. Ghodssi and P. Lin (Springer, New York, 2011), Chap. 8, pp. 457–665.